

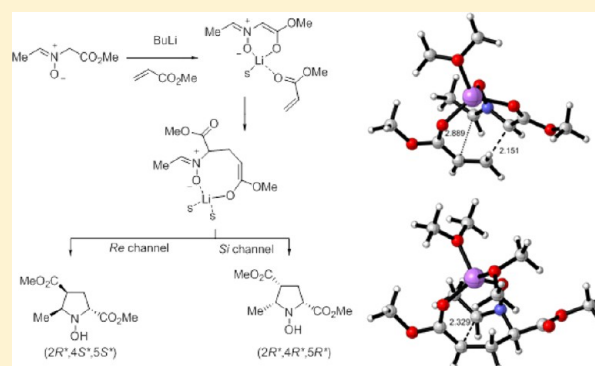
Theoretical Elucidation of the Mechanism of the Cycloaddition between Nitron Ylides and Electron-Deficient Alkenes

P. Merino,* T. Tejero, and A. Díez-Martínez

Laboratorio de Síntesis Asimétrica, Departamento de Síntesis y Estructura de Biomoléculas, Instituto de Síntesis Química y Catálisis Homogénea (ISQCH), Departamento de Química Orgánica, Universidad de Zaragoza, CSIC, E-50009 Zaragoza, Aragón, Spain

S Supporting Information

ABSTRACT: A full theoretical study of the reaction between a novel type of ylide, i.e. nitron ylides, and alkenes has been carried out. Both concerted and polar stepwise mechanisms have been considered. Only the zwitterionic mechanism predicts correctly the experimentally observed adducts. Depending on the level of theory, the mechanism moves from concerted to polar stepwise, as demonstrated by the corresponding IRC analyses. The regio- and stereoselectivity of the reaction is well explained for both mono- and disubstituted alkenes. In the case of methyl acrylate a pathway leading to the two diastereoisomers obtained experimentally is predicted. For methyl fumarate a stereospecific mechanism is predicted as a consequence of a C–H⋯O=C interaction present in a Li-tricoordinated transition structure. The stereospecificity in the reaction with methyl maleate comes from a less hindered coordination around the lithium atom. Calculations with B3LYP and M06-2X functionals indicate that only the latter provides energy values in good agreement with experimental findings.



INTRODUCTION

Cycloaddition reactions are not necessarily pericyclic.¹ Some discussion has occurred in the past concerning classical cycloadditions such as Diels–Alder reactions, dipolar cycloadditions, and related processes directed at considering the possibility of stepwise biradical mechanisms.² In several cases, the biradical process has shown to be favored with respect to the corresponding concerted mechanism; this is the case, for instance, of some Diels–Alder reactions³ and the dimerization of nitrile oxides.⁴ Alternatively, pseudopericyclic reactions have been defined by Birney and co-workers as a novel approach to explain apparently disallowed pericyclic reactions.⁵ Intermediate situations have been reported by Houk and co-workers,⁶ and recently, we have reported a variation that could be considered as a bipseudopericyclic process.⁷ Cycloadditions can also take place through a polar stepwise mechanism.⁸ Indeed, typical concerted reactions can move to a polar mechanism on catalysis with Lewis acids.⁹ Accordingly, there have been reported a variety of relevant studies considering concerted vs stepwise mechanisms (both biradical and polar) for a series of cycloaddition reactions.¹⁰

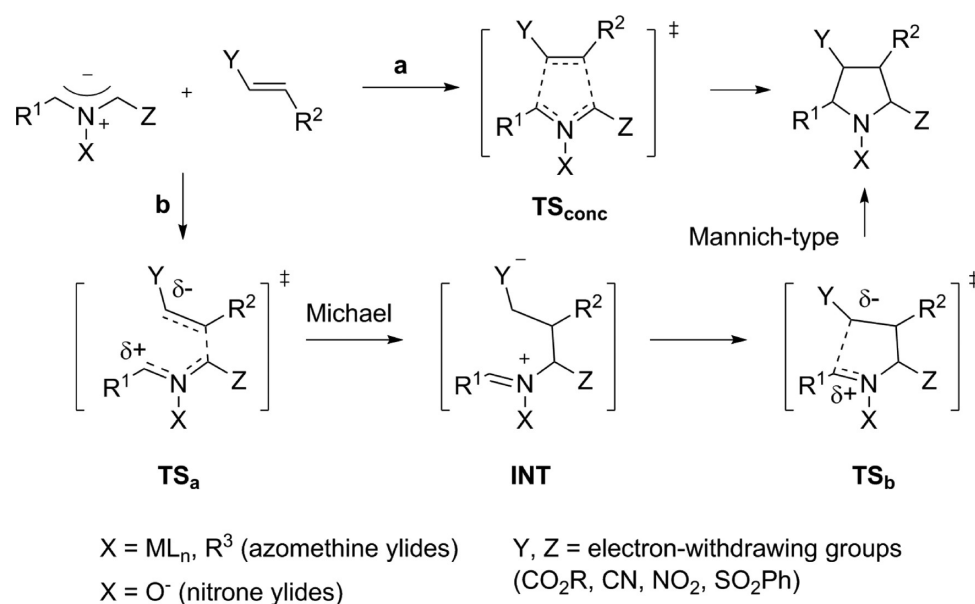
Experimental proofs have been found in several cases by isolating and trapping intermediates,^{9d,11} and in many other situations theoretical calculations fully supported the stepwise vs the concerted process.^{3,8b–g} Dipolar cycloadditions of azomethine ylides are representative of a dual situation. Depending on the substrates and/or the catalysts a concerted mechanism (Scheme 1, path a) or a stepwise mechanism (Scheme 1, path b) operates. Domingo et al. reported a concerted mechanism for

trifluoromethyl thiomethyl azomethine ylides supported by DFT calculations¹² although ELF analysis showed that the reaction was not pericyclic.¹³ A concerted mechanism has also been invoked for the reaction between azomethine ylides and simple substituted alkenes¹⁴ as well as for organocatalyzed reactions.¹⁵ On the other hand, Cossio and co-workers demonstrated a stepwise mechanism for the reaction of azomethine ylides with nitroalkenes by detecting an intermediate by NMR spectroscopy.¹⁶ The stepwise process was also supported by DFT calculations, as in the case of a cycloaddition catalyzed by silver and copper complexes reported by Najera and co-workers.¹⁷ Moreover, Carretero and co-workers demonstrated the capability of azomethine ylides of behaving as nucleophiles (the first step of a stepwise cycloaddition) in the addition of such compounds to imines through a Mannich-type reaction.¹⁸ Isolation of intermediate Michael-type addition compounds at lower temperatures and further DFT calculations supported the stepwise mechanism.¹⁹

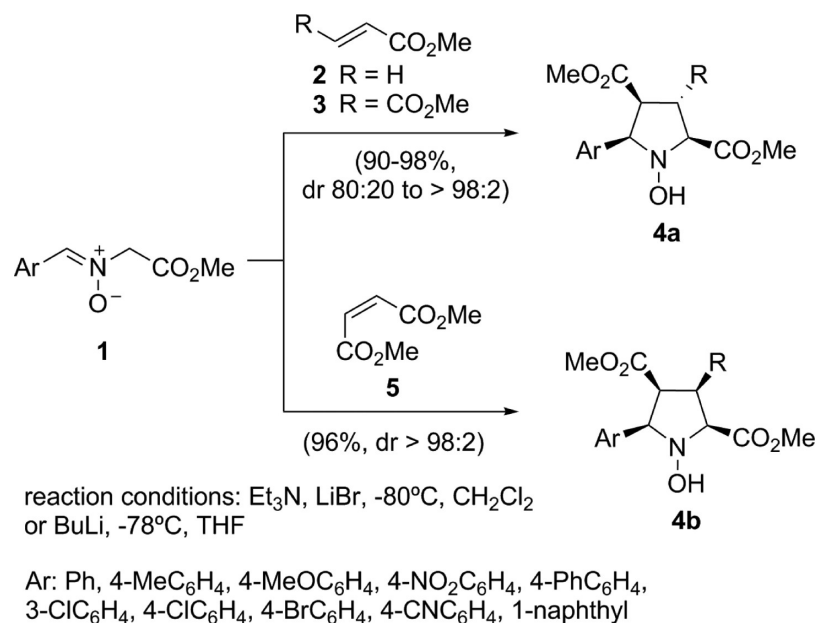
In this context, we have recently reported a full experimental study on a new and different sort of ylide: i.e., nitron ylides (Scheme 2).²⁰ Although they could be considered close to azomethine ylides because the only difference resides in the oxygen atom replacing the carbon/metal atom attached to the nitrogen, their electronic structure is completely different. Nitrones are well-known dipoles in 1,3-dipolar cycloadditions²¹

Received: January 10, 2014

Published: February 18, 2014

Scheme 1. Concerted (a) and Stepwise Polar (b) Mechanisms for Cycloadditions of Azomethine Ylides ($X = ML_n, R^3$) and Nitronyl Ylides ($X = O^-$)

Scheme 2. Diastereoselective Cycloaddition between Nitronyl Ylides and Electron-Deficient Alkenes



toward the synthesis of nitrogenated heterocycles including pyrrolidines.²² Nitrones can also behave as electrophiles in organometallic additions²³ and stepwise cycloadditions with electron-rich alkenes, as we have recently demonstrated for Mannich-type reactions with silyl ketene acetals.^{8e,g,9e}

In the case of nitronyl ylides the oxygen atom does not participate in the reaction and a different approach should be considered. In our previous experimental paper we isolated an open-chain intermediate for the reaction with methyl acrylate, demonstrating that the reaction followed a stepwise mechanism. On the other hand, we were not able to isolate the corresponding intermediate in the case of disubstituted alkenes (dimethyl maleate and fumarate). Since the stereochemistry of the alkene was conserved and the reaction was shown to be stereospecific, this might indicate that a concerted mechanism could operate in

the case of disubstituted alkenes. To shed some light on the mechanism of this reaction, the cycloaddition of nitronyl ylides with electron-poor alkenes, we have carried out a full theoretical study of the reaction considering both mono- and disubstituted alkenes. In this paper we report our results on that study.

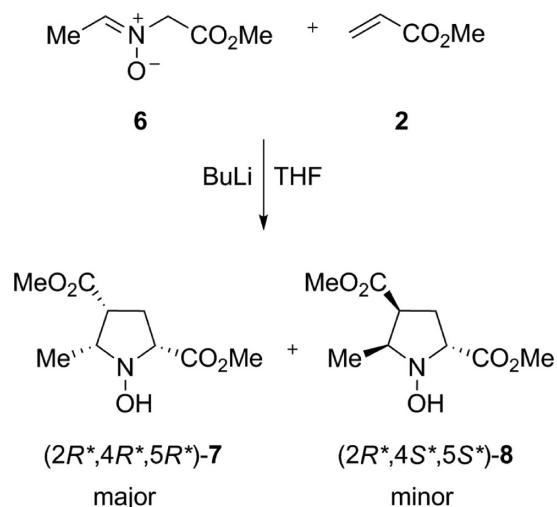
■ COMPUTATIONAL METHODOLOGY

Computations with density functional theory (DFT) were carried out using the exchange-correlation functional B3LYP²⁴ and Truhlar's functional M06-2X.²⁵ The standard basis sets 6-31G(d) and 6-311G(d,p) were employed, and diffuse functions were added in both cases.²⁶ The nature of stationary points was defined on the basis of calculations of normal vibrational frequencies (force constant Hessian matrix). The optimizations were carried out using the Berny analytical gradient optimization method.²⁷ Minimum energy pathways for the reactions studied were found by gradient descent of transition states in

the forward and backward direction of the transition vector (IRC analysis),²⁸ using the second-order González–Schlegel integration method.²⁹ The solvent effects modeled as a continuum model were considered for single points and fully optimized highest level of theory employed using a relatively simple self-consistent reaction field (SCRFF³⁰) based on the polarizable continuum model (PCM) of Tomasi's group.³¹ The electronic energies in solution were obtained by adding the total electrostatic energies obtained from the PCM calculations to the electronic energies in vacuo. The PCM and solvent = THF options were employed in the SCRFF calculations, in which solvent effects have been considered. In addition, microsolvation of the lithium atom was considered by adding discrete molecules of dimethyl ether surrounding the lithium atom.³² Single-point calculations were also carried out using B3LYP/6-31+G(d) geometries. Thus, for the purpose of comparison the following levels of theory were calculated: (i) B3LYP/6-31+G(d); (ii) M06-2X/6-31+G(d); (iii) PCM=THF/B3LYP/6-311+G(d)//B3LYP/6-31+G(d); (iv) PCM=THF/M06-2X/6-311+G(d)//B3LYP/6-31+G(d); (v) PCM=THF/M06-2X/6-311+G(d). Open-shell calculations (UM06-2X/6-31+G(d)) were also carried out, and results identical with those obtained with closed-shell calculations were found, thus confirming that no biradical mechanism is competing with the proposed zwitterionic mechanism. All calculations were carried out with the Gaussian 09 suite of programs.³³ Structural representations were generated using CYLview.³⁴

All of the discussions will be based on the highest level used (PCM=THF/M06-2X/6-311+G(d)). References to the other levels, whose values are provided in the Supporting Information, will be made when notable differences have been observed. Consistent with our previous experimental report, we have studied the reaction between nitron 6 and methyl acrylate 2 to give *N*-hydroxypyrrrolidines 7 and 8 with 2*R**,4*R**,5*R** and 2*R**,4*S**,5*S** relative configurations,³⁵ respectively, in the presence of butyllithium in THF as a solvent (Scheme 3).

Scheme 3. Cycloaddition Reaction between 6 and 2



RESULTS AND DISCUSSION

The first irreversible step of the reaction illustrated in Scheme 3 is the proton abstraction in nitron 6 by butyllithium to form the corresponding nitron ylide 9 (Scheme 4). Once the ylide is formed, two different approaches can be considered: (i) a direct approach (Scheme 4, path a) through the concerted transition state TS-c leading to the final product PR and (ii) an initial Michael attack (Scheme 4, path b) of the nitron ylide to methyl acrylate 2 through TS-s1 to form intermediate IN1, followed by an intramolecular Mannich-type reaction through TS-s2 to yield the product PR.

Direct Approach. There are three possible initial transition states for a direct approach of methyl acrylate 2 to ylide 9, corresponding to three alternate dispositions of the two reagents (one antiperiplanar and two gauche). This makes a total of 12 possible approaches to be calculated, since two faces are possible for the planar acrylate and two conformations (*s-cis* and *s-trans*) are possible for the same compound. From these 12 orientations, 4 of them corresponding to gauche orientations could lead to concerted transition states TS1–TS4 (Figure 1). From the other 8 approaches we discarded 4 of them because they present significant unfavorable steric interactions. From the remaining four transition structures TS5–TS8 only one did not present favorable interactions between the lithium atom and the carbonyl oxygen. Thus, we located the eight transition structures TS1–TS8 illustrated in Figure 1.

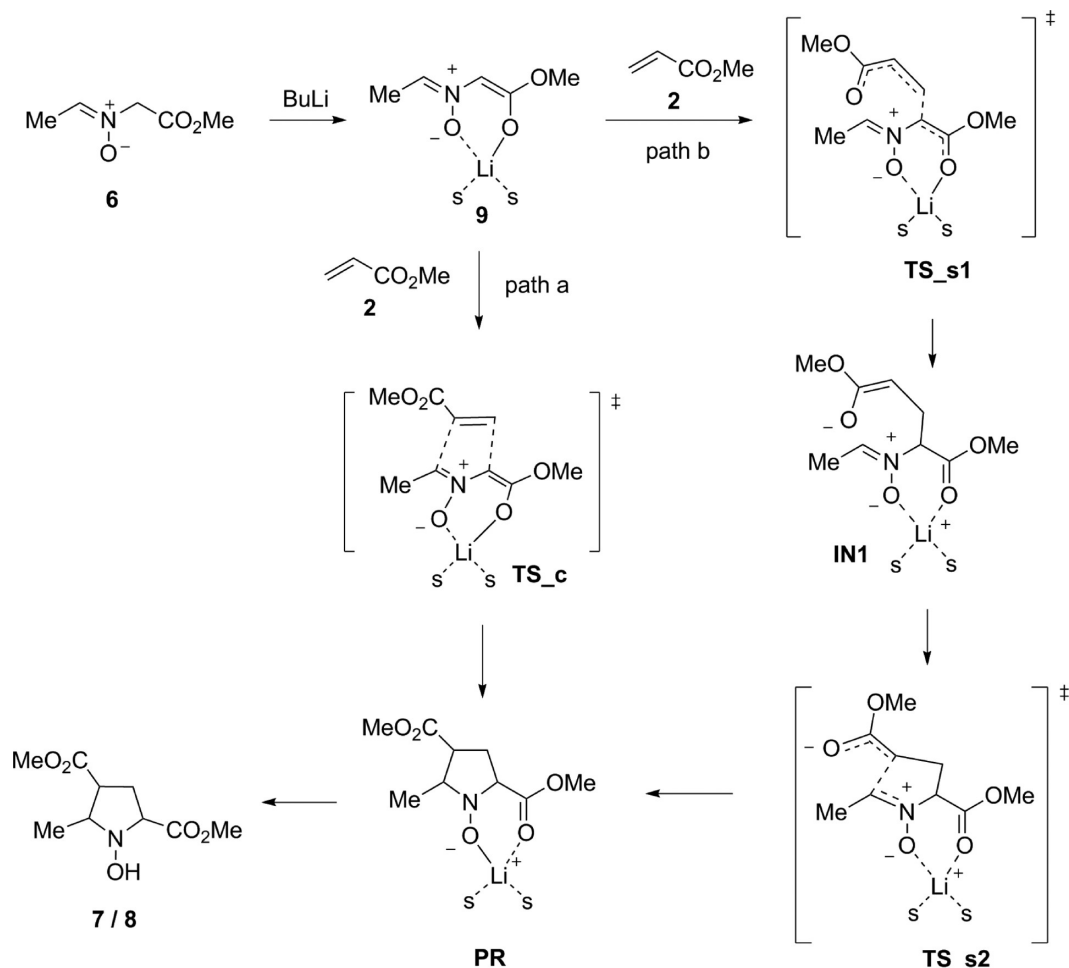
All of the levels of theory studied showed TS1 and TS3 as the most stable, having enough energy differences (more than 3 kcal/mol) to exclude the rest of the TSs. The endo approach corresponding to TS1 is the most stable for all the levels studied, with the exception of the highest level, which showed TS3 to be 0.5 kcal/mol more stable than TS1. In this level, the calculated energy barriers for TS1 and TS3 were 14.7 and 14.2 kcal/mol, respectively. The geometries of TS1 and TS3 are given in Figure 2.

The forming C2–C3 bonds have lengths of 2.066 and 2.079 Å for TS1 and TS3, respectively. The distances between C4 and C5 are 2.988 and 2.902 Å for TS1 and TS3, respectively. These data point to a very asynchronous concerted reaction. However, the frequency analysis—regarding the only imaginary frequency found for such TSs—was not definitive to identify the reaction as concerted. The corresponding IRC analysis for TS3 at the M06-2X/6-31+G(d) level showed a concerted process starting with the reagents (nitron ylide 9 and methyl acrylate 2) and ending with the corresponding coordinated *N*-hydroxypyrrrolidine.³⁶ On the other hand, an identical IRC analysis for TS1 at the same level of theory showed 9 and 2 as the starting point but IN1 as the final one. Moreover, although TS3 leads to the major isomer 2*R**,4*R**,5*R** observed experimentally, TS1 predicted the obtention of 2*R**,4*S**,5*R** isomer 10, whereas the minor isomer observed experimentally was compound 8, having the 2*R**,4*S**,5*S** configuration (Scheme 5). At this point, it was evident that the direct approach cannot be considered as the correct one. Notably, IRC analyses of both TS1 and TS3 at the highest PCM=THF/M06-2X/6-311+G(d,p) level showed the reaction as a stepwise process ending in the corresponding intermediate IN1.³⁶ Accordingly, the interaction between C4 and C5 in the transition states leading to distances of 2.988 and 2.902 Å can be considered as strictly electrostatic, and it does not represent a forming bond, in agreement with the previously reported anionic stepwise [3 + 2] cycloadditions.³⁷

With this result in hand, it is possible to conclude that the reaction is stepwise and further evolution of intermediate IN1 should involve the coordination of the formed enolate to the lithium atom through exchange of (i) a solvent molecule to form intermediate IN2 (Figure 3), (ii) the other ester carbonyl to form IN3, or (iii) the nitron oxygen to form IN4. Among these complexes IN4 can be discarded, since for the second step, consisting of an intramolecular Mannich-type addition, activation of the nitron by means of lithium coordination is required, as we demonstrated both experimentally and theoretically.^{8e,9e}

At this point, it seems more plausible that coordination between methyl acrylate and the lithium atom takes place before

Scheme 4. Concerted and Stepwise Mechanisms for the Cycloaddition of Nitronyl Ylide 9 with Methyl Acrylate 2 (s = Solvent)



the initial Michael addition, thus increasing the electrophilicity of the Michael acceptor. This approach, discussed in the next section, will allow an explanation of not only the formation of intermediates **IN2** and **IN3** but also their further cyclization as well as the observed experimental results.

Stepwise Mechanism. Previous work from this laboratory³⁸ demonstrated that nucleophilic additions of organometallic reagents to nitrones take place through the formation of an initial complex between the nitronyl and the organometallic reagent.³⁹ Moreover, it has also been demonstrated that coordination of the metal atom to the nitronyl oxygen is required in order to increase the electrophilic character of the nitronyl carbon.^{9c} In a similar way, and advancing a second step consisting of a Mannich-type addition to nitronyls^{8g} (see below), it is possible to consider the initial formation of complex **11** between ylide **9** and methyl acrylate **2** (Scheme 6, R = H). The formation of complex **11** takes place without an energy barrier and activates the double bond toward the initial Michael attack. This complex leads to intermediate **IN2** through **TS9**, in which the lithium atom is kept coordinated to both ester moieties as well as the nitronyl oxygen. Further evolution of **IN2** toward the product is rather limited because of the rigidity of the model. Thus, transformation of **IN2** into **PR1**, a precursor of the major product observed experimentally, is only possible through **TS10**. We located all the stationary points illustrated in Scheme 6. A full energy diagram is given in Figure 4. Notably, **TS9** is 5.5 kcal/mol lower in energy than **TS3**, thus demonstrating that the pathway illustrated in

Scheme 6, involving previous coordination of methyl acrylate, is preferred.

The activation free energy associated with the conversion of the reagents into **IN2** is 8.7 kcal/mol. The intermediate **IN2** is located 0.3 kcal/mol below the reagents, and the energy barrier for the second step of the reaction is 13.3 kcal/mol to form the adduct **PR1**, which is located 15.7 kcal/mol below the reagents. Consequently, the rate-limiting step for this process is the intramolecular Mannich-type reaction.

The geometries of **TS9** and **TS10** are given in Figure 5. The length of the forming C2–C3 bond in **TS9** is 2.151 Å. Also in this case an interaction between C4 and C5 is observed, with a distance of 2.889 Å. Again the IRC analysis for **TS9** confirmed that the final forward point of this step was **IN2** (see the Supporting Information) with a C2–C3 bond length of 1.585 Å and a distance between C4 and C5 of 3.320 Å. The length of the forming C4–C5 bond in **TS10** is 2.330 Å, in good agreement with those previously observed for intermolecular Mannich-type additions of lithium ester enolates to nitronyls.^{8c} The coordination of the lithium atom to the three oxygen atoms during the rate-limiting step is responsible for the all-cis relative configuration observed experimentally for the major adduct **7**. However, such coordination does not allow any other approach of the ylide to the nitronyl moiety because of the rigidity of the system. Consequently, the path involving **TS10** cannot justify the obtention of the minor adduct **8**, predicting a completely stereoselective reaction (Figure 4, blue path). On the other hand,

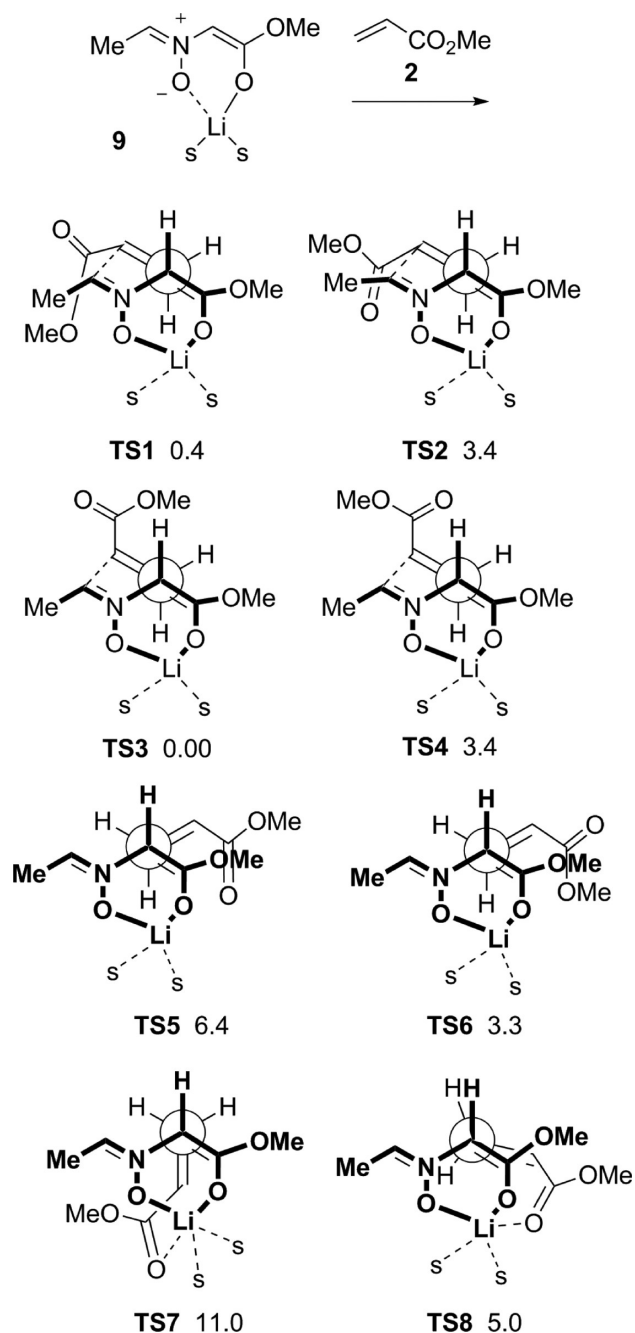


Figure 1. Transition structures corresponding to the direct approach between nitronylide **9** and methyl acrylate **2** (relative free energies calculated at the PCM=THF/M06-2X/6-311+G(d,p) level of theory are indicated in kcal/mol).

intermediate **IN3** has enough flexibility for considering two competitive approaches of the enolate by the two faces of the nitronylide. Both **IN2** and **IN3** are connected by a solvent molecule exchange, the formation of **IN3** from **IN2** being exothermic by 6.0 kcal/mol. This difference in energy is justified by the incorporation of an additional solvent molecule (in agreement with previous studies),⁴⁰ liberating strain in the lithium coordination.

The intermediate **IN3** evolves through diastereomeric *Si* and *Re* channels to give adducts **PR2** and **PR3**, respectively. This pathway is in full agreement with the observed experimental results, since it predicts the two observed adducts having

$2R^*$, $4R^*$, $5R^*$ and $2R^*$, $4S^*$, $5S^*$ configurations. The geometries of the corresponding **TS11** and **TS12** are given in Figure 5. The lengths of the forming C4–C5 bond at **TS11** and **TS12** are 2.299 and 2.329 Å, respectively. The analysis of the free activation energies revealed that **TS11** is favored by 0.5 kcal/mol. The energy barriers are 10.1 and 10.6 kcal/mol lower in energy than that associated with the direct conversion of **IN2** into **PR1** via **TS10**. The formation of **IN3** leads to a competitive obtention of **7** and **8**, predicting diastereomeric mixtures as occurs experimentally. By consideration of this path, i.e. interconversion of **IN2** into **IN3**, the rate-determining step corresponds to that in which the first C2–C3 bond is formed (**TS9**).

From the several levels of theory studied, only those using Truhlar's functional M06-2X provided energy values in agreement with the experimental findings for an exergonic reaction. Energy calculations with the B3LYP functional (B3LYP/6-31+G(d)) predict an endergonic reaction. On the other hand, both calculations in the absence of solvent (M06-2X/6-31+G(d)) and fully optimized triple- ζ calculations (PCM=THF/M06-2X/6-311+G(d,p)) using Truhlar's functional afforded results coherent with the experimental observations. The differences between functionals are also evidenced in single-point calculations using B3LYP geometries. Whereas the B3LYP functional (PCM=THF/B3LYP/6-311+G(d,p)//B3LYP/6-31+G(d)) predicts again an endergonic reaction, the M06-2X functional (PCM=THF/M06-2X/6-311+G(d,p)//B3LYP/6-31+G(d)) provides results quite similar to those obtained with the highest level of theory employed (see the Supporting Information).

Cycloaddition with Disubstituted Alkenes. The reaction of nitronylide with methyl fumarate **3** only afforded one isomer in all cases studied.²⁰ The obtained isomers have a $2R^*$, $3R^*$, $4R^*$, $5R^*$ configuration (Scheme 6, compound **13**). In order to evaluate if the same mechanism operating for methyl acrylate **2** could be valid for disubstituted alkenes, we studied the reaction following the same methodology described in the preceding section. Calculations at the PCM=THF/M06-2X/6-311+G(d,p) level of all the stationary points illustrated in Scheme 6 (R = CO₂Me) were carried out. In addition, the corresponding transition structures equivalent to **TS1** and **TS3** were also located, showing in both cases values higher in energy than for **TS13**, the corresponding transition structure for the initial Michael addition (for details see the Supporting Information). A full energy diagram is given in Figure 6. The geometry of **TS13** is given in Figure 7. The length of the forming C2–C3 bond is 2.085 Å, and an interaction between C4 and C5 is observed with a distance of 2.749 Å. The IRC analysis of **TS13** led to the same conclusion as that in the case of **TS9** for methyl acrylate, the final forward point being **IN5**. Thus, also in the case of methyl fumarate the reaction follows a stepwise mechanism. However, some important differences are appreciated in the energy diagram illustrated in Figure 6. The formation of the first intermediate **IN5** through the initial Michael addition is the rate-limiting step of the reaction, as in the case of methyl acrylate. The energy barrier is 5.3 kcal/mol. The corresponding intermediate **IN5** is 3.3 kcal/mol below the reagents. Also, the intermediate **IN6** is thermodynamically favored by 4.8 kcal/mol. However, in contrast to what is observed for methyl acrylate, the transition structure **TS14** coming from the monosolvated intermediate **IN5** is lower in energy than the transition structures **TS15** and **TS16** coming from the disolvated **IN6**. A close look at **TS14** reveals that an additional hydrogen bond between the C–H in the α position of the nitronylide nitrogen and the carbonyl group at

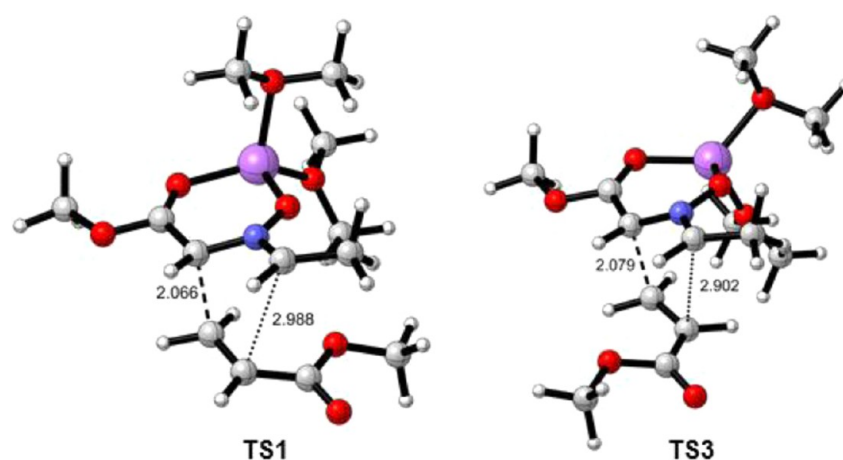


Figure 2. Transition structures corresponding to the direct approach between nitron ylide **9** and methyl acrylate **2** optimized at the PCM=THF/M06-2X/6-311+G(d,p) level of theory (distances given in angstroms).

Scheme 5. Predicted Products for a Concerted Mechanism and Those Observed Experimentally

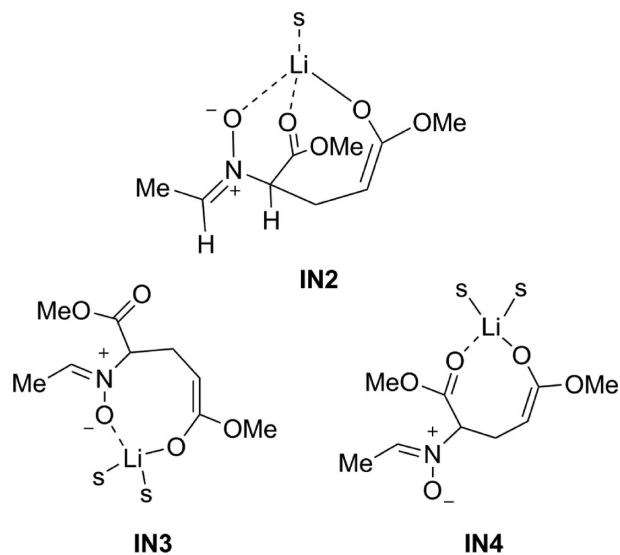
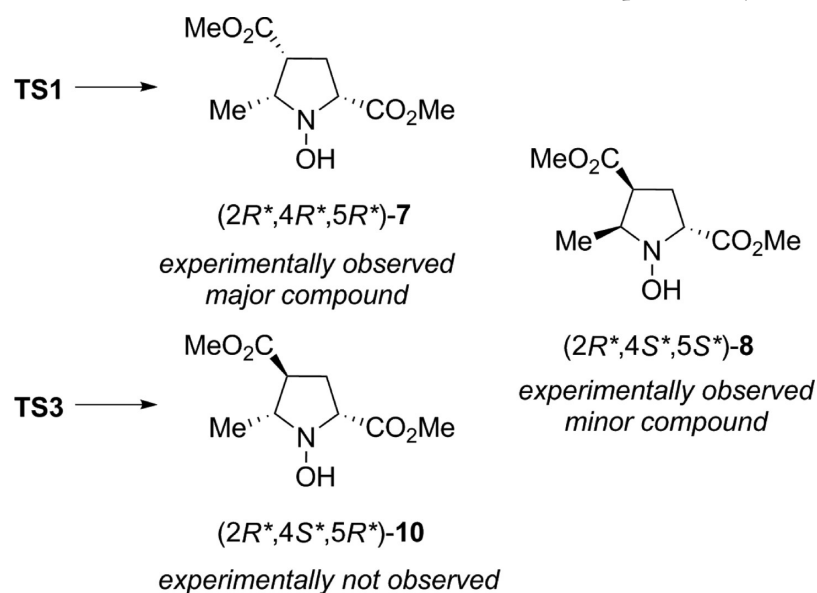
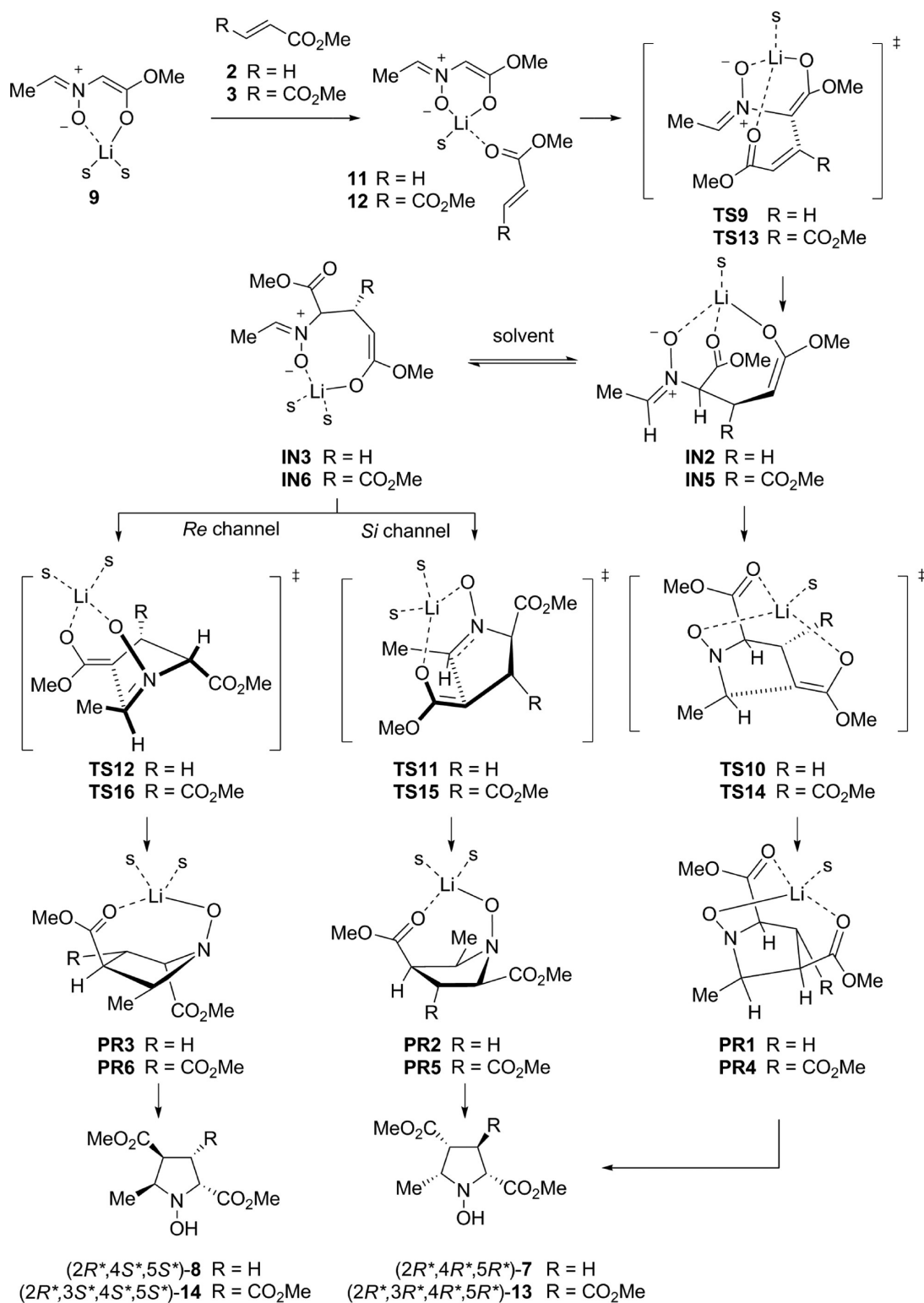


Figure 3. Plausible intermediates in the stepwise mechanism.

the noncoordinated ester group exists in comparison with **TS10**. That C–H⋯O=C interaction (2.441 Å) justifies the stabilization of **TS14** with respect to **TS10**, since it contributes to increasing the electrophilicity of the nitron carbon. Since both TSs (**TS10** and **TS14**) have very similar geometries, it is possible to conclude that the nature of the stabilization of **TS14** with respect to **TS10** is electronic and not steric. Further support for this hypothesis has been obtained from additional calculations. Upon replacement of the ester group by a nitro group, the same interaction is observed and a similar stabilization is predicted. On the other hand, upon replacement of the ester group by a methyl group no stabilization is observed—as in the case of methyl acrylate (**TS10**)—since no interaction is possible (for details see the Supporting Information).

Consequently, for the reaction of nitron ylide **9** with methyl fumarate **3**, the preferred pathway is that in which the lithium atom is tricoordinated, only being possible for the formation of adduct **13** (Figure 6, black path). These results fully explain the complete stereoselectivity observed experimentally. The geometries of **TS14**–**TS16** are given in Figure 7, which are very similar to those found for methyl acrylate (**TS10**–**TS12**). The

Scheme 6. Stepwise Mechanisms for the Cycloaddition of Nitrone Ylide 9 with Methyl Acrylate 2 and Methyl Furmarate 3 ($s = \text{Me}_2\text{O}$)

lengths of the forming C4–C5 bond in **TS14**–**TS16** are 2.312, 2.312, and 2.310 Å, respectively.

The reaction between **9** and methyl maleate **5** also afforded a single diastereomer having the $2R^*,3S^*,4R^*,5R^*$ configuration. However, it presents notable differences with respect to the reaction between **9** and **3** as a consequence of the *Z* configuration of the double bond. The presence of a second ester unit oriented

toward the lithium atom shows that additional models of coordination could be possible. The considered stepwise mechanisms are illustrated in Scheme 7, and a full diagram is given in Figure 8. We have also located **TS3''**, the lowest transition structure corresponding to a direct approach between **9** and **5**. The energy barrier for such an approach is 10.8 kcal/mol (Figure 8, red pathway). The first step of the reaction is similar to

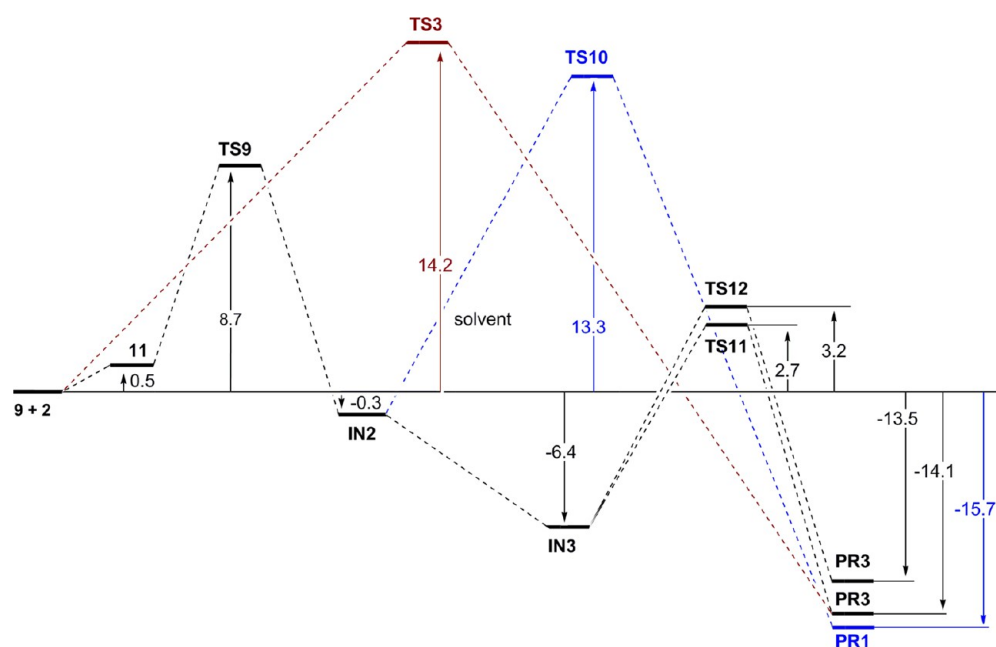


Figure 4. Energy diagram for the stepwise mechanisms corresponding to the cycloaddition of nitron ylide 9 with methyl acrylate 2 (Scheme 6, R = H). Relative energy values are given in kcal/mol and correspond to optimized points at the PCM=THF/M06-2X/6-311+G(d,p) level.

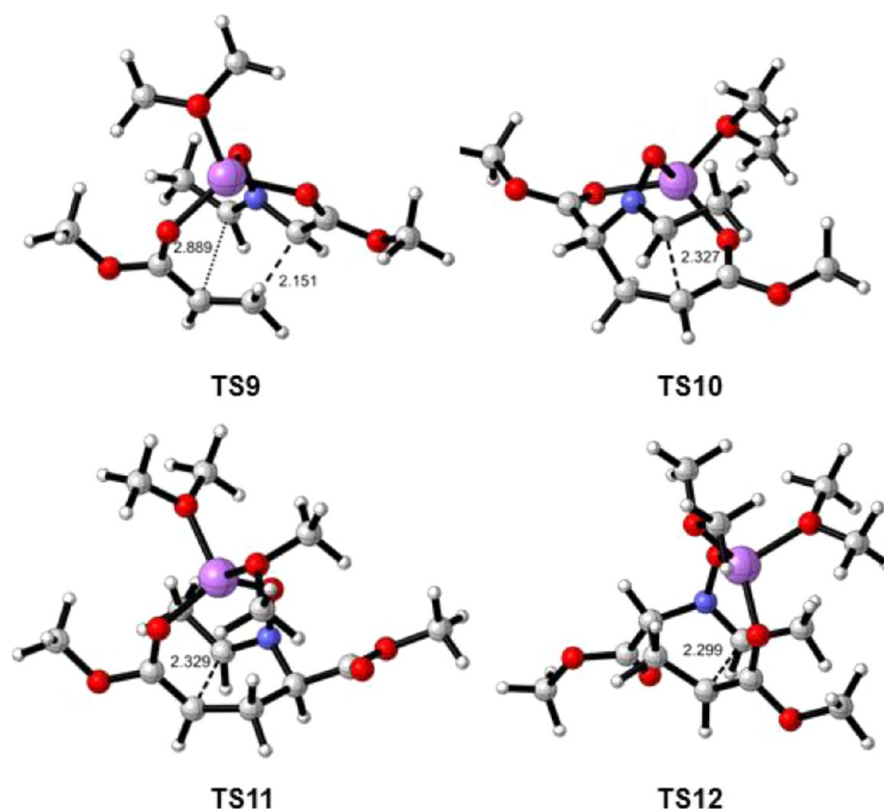


Figure 5. Geometry of transition structures TS9–TS12 at the PCM=THF/M06-2X/6-311+G(d,p) level.

that observed for 2 and 3, since coordination of the carbonyl oxygen at the β position is required to promote the Michael addition. Thus, complex 15 evolves toward intermediate IN7 through TS17. The energy barrier for this transformation is 7.8 kcal/mol, since 15 is 1.3 kcal/mol above the reagents (nitron ylide and alkene). The geometry of TS17 is given in Figure 9. The forming bond C2–C3 is 2.085 Å, and the interaction between C4 and C5 afforded a distance of 2.749 Å between those

atoms. The IRC analysis of TS17 clearly demonstrates that it connects 15 with IN7. This intermediate can be transformed into PR7, the precursor of the only obtained $2R^*,3S^*,4R^*,5R^*$ isomer, through TS18 with an energy barrier of 4.8 kcal/mol. Notably, PR7 is the most stable complex, in which no solvent molecules are coordinated to the lithium atom. Other complexes having one solvent molecule coordinated were shown to be less stable. The forming bond C4–C5 in TS18 is 2.304 Å (Figure 9).

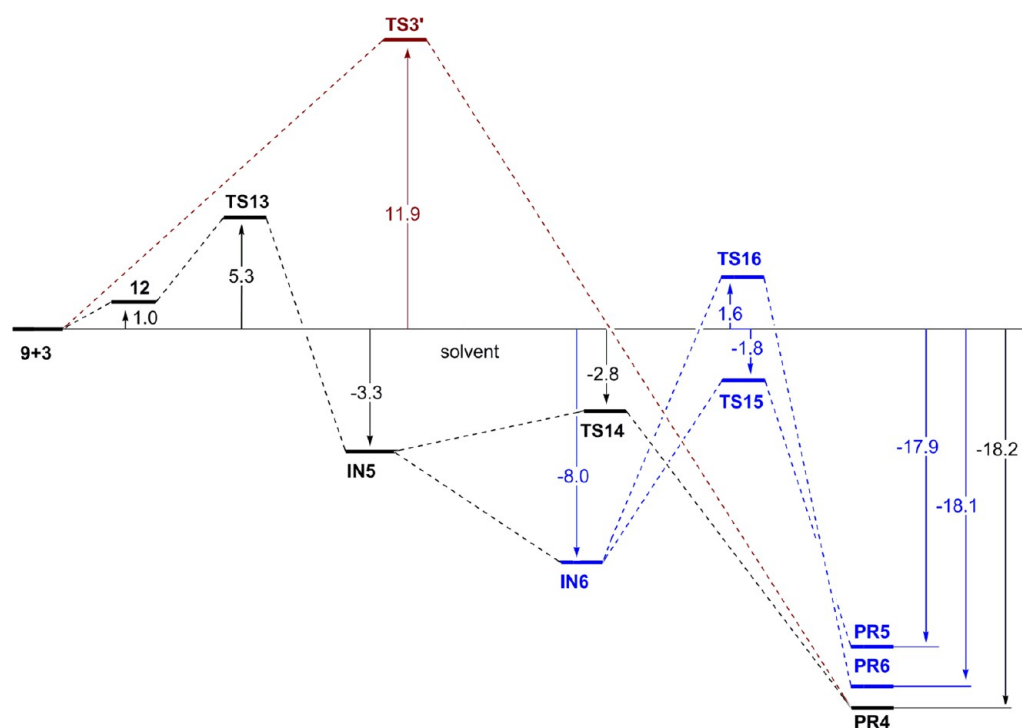


Figure 6. Energy diagram for the stepwise mechanisms corresponding to the cycloaddition of nitron ylide **9** with methyl fumarate **3** (Scheme 6, R = CO₂Me). Relative energy values are given in kcal/mol and correspond to optimized points at the PCM=THF/M06-2X/6-311+G(d,p) level.

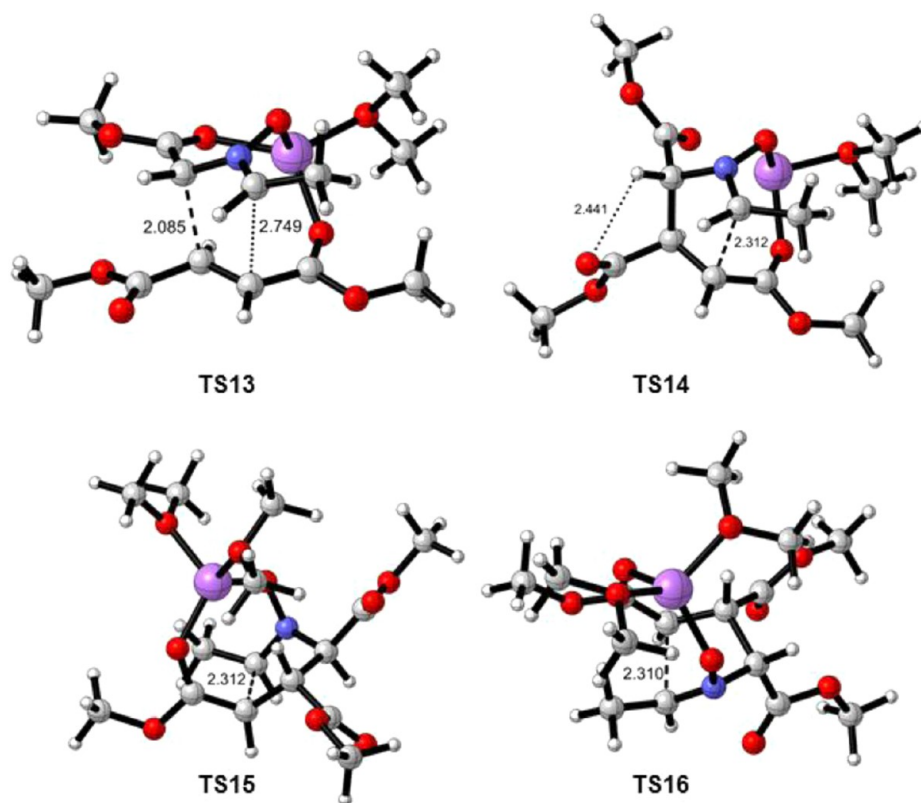
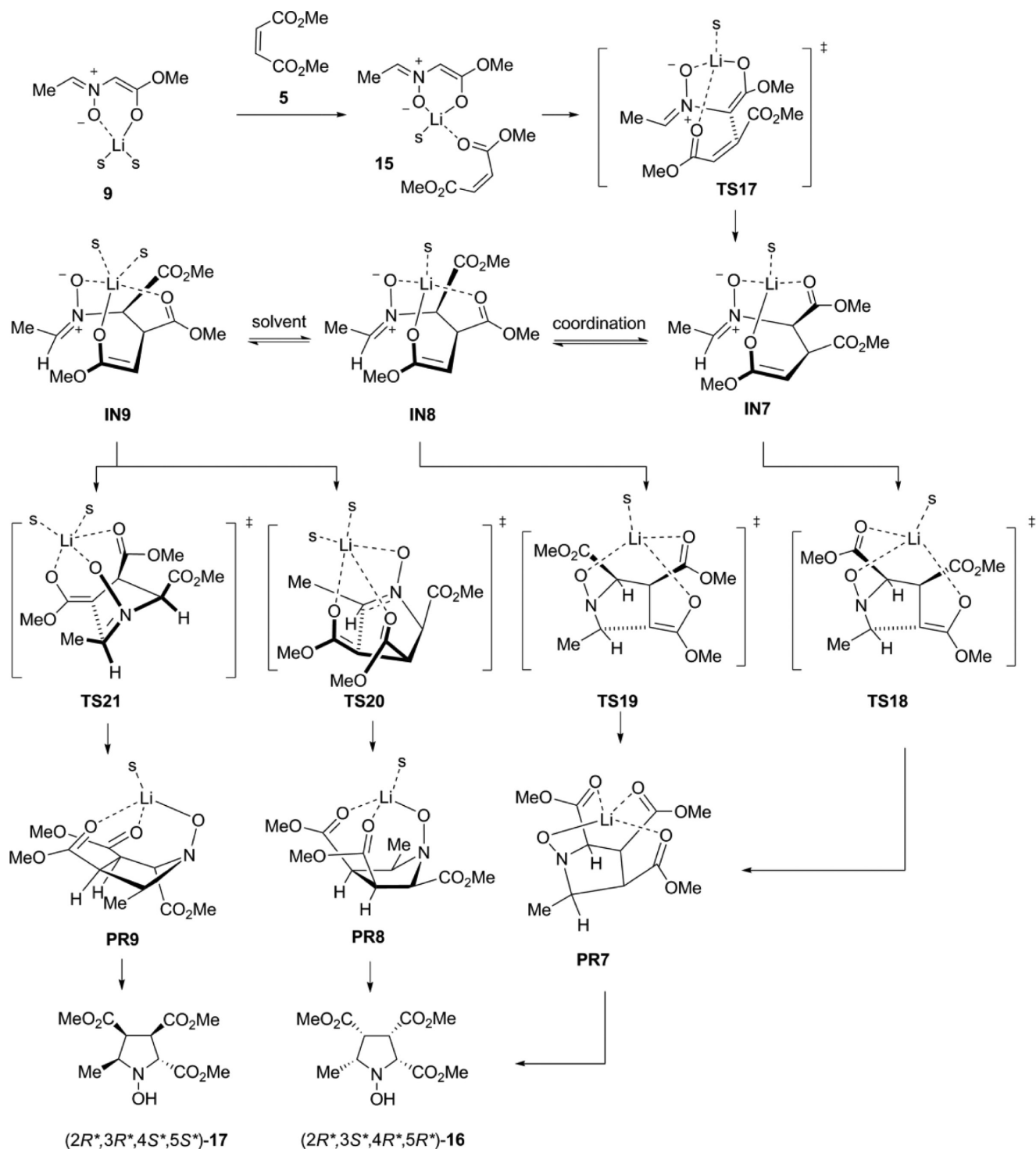


Figure 7. Geometry of transition structures TS13–TS16 at the PCM=THF/M06-2X/6-311+G(d,p) level.

Coordination in IN7 exerts a high strain; indeed, this intermediate is 0.5 kcal/mol above the reagents. On the other hand, exchange of coordination with the ester at the β position of the nitron nitrogen afforded the considerably more stable IN8, which is 11.8 kcal/mol below the reagents. IN8 can also be

converted into PR7 through TS19, which is 1.9 kcal/mol below the reagents. The forming bond C4–C5 in TS19 is 2.312 Å (Figure 9). As in the case of methyl fumarate and acrylate we also considered exchange of the ester coordination by a solvent molecule. However, in this case the relative configuration of the

Scheme 7. Stepwise Mechanisms for the Cycloaddition between Nitrone Ylide 9 and Methyl Maleate 5 ($s = \text{Me}_2\text{O}$)

ester group at the β position of the nitrone nitrogen favors the proximity to the lithium atom and pentacoordinated lithium is obtained as the most stable complex, where two molecules of solvent are considered. Coordination of the ester at the α position of the nitrone nitrogen is disfavored as illustrated in IN7. The corresponding intermediate IN9 is less stable than IN8, being 5.3 kcal/mol below the reagents. We considered the two possible Mannich-type attacks in IN9 leading to PR8 and PR9 through TS20 and TS21, respectively. Whereas TS21 leading to the not experimentally observed isomer 15 is 0.1 kcal/mol below

the reagents, TS20 leading to the obtained 14 is found to be considerably less stable, being 7.4 kcal/mol above the reagents. The lengths of forming bonds C4–C5 in TS20 and TS21 are 2.312 and 2.310 Å, respectively (Figure 9).

From these results it becomes evident that in the case of methyl maleate the preferred route is the formation of IN8 through TS17 and IN7, followed by transformation into PR7 through TS19 (Figure 8, black path). The stabilization of TS19 with respect to TS18 is due to the different coordination around the lithium atom. Whereas in TS18 (as in TS10 and TS14)

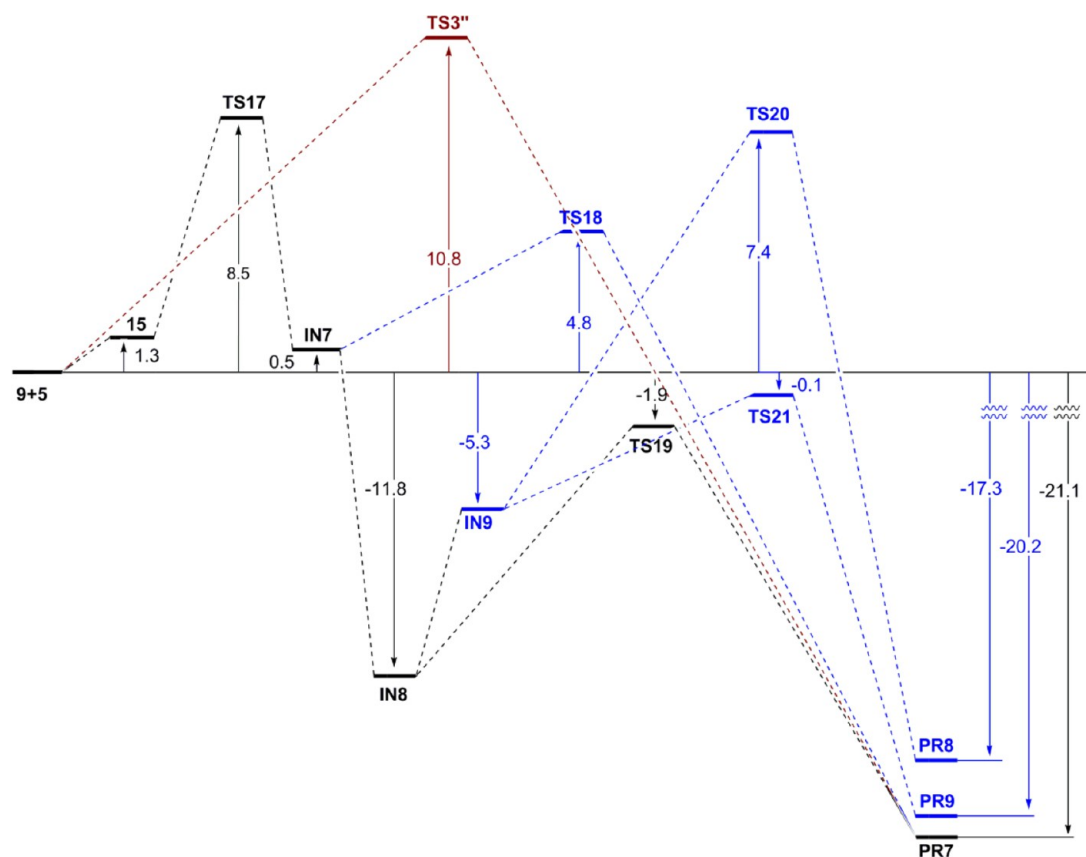


Figure 8. Energy diagram for the stepwise mechanisms corresponding to the cycloaddition of nitronylide **9** with methyl maleate **5**. Relative energy values are given in kcal/mol at the PCM=THF/M06-2X/6-311+G(d,p) level.

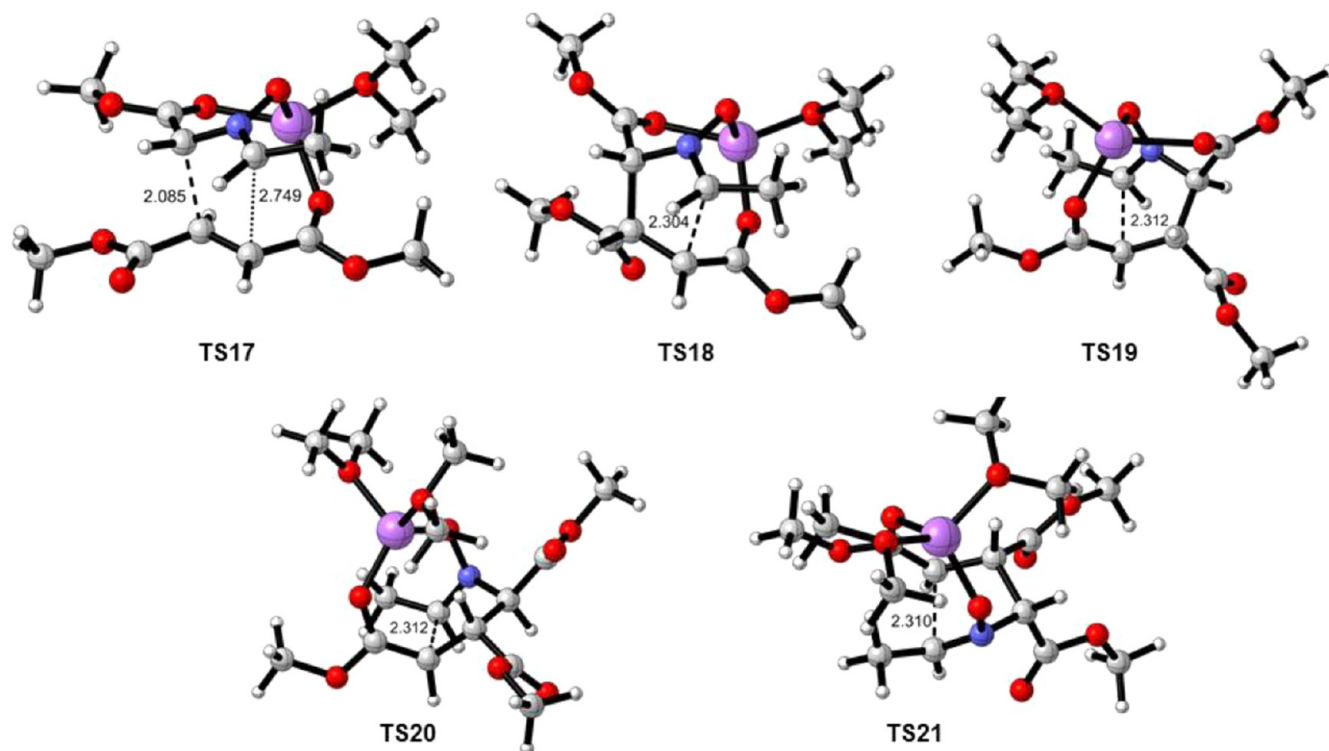


Figure 9. Geometry of transition structures TS17–TS21 at the PCM=THF/M06-2X/6-311+G(d,p) level.

coordination of the ester group at the α position of the nitronylide nitrogen leads to a O–Li–O angle of 89.9° , in the case of TS19

coordination of the ester group at the β -position of the nitronylide nitrogen leads to a O–Li–O angle of 106.3° , much closer to a

tetrahedral disposition around the lithium atom. This is also the ultimate reason for the stabilization of **TS19** with respect to **TS10**, since in **TS19** the stabilizing C–H...O=C interaction observed in **TS14** is not possible. Consequently, in this case, it is possible to conclude that the nature of the stabilization of **TS19** with respect to **TS10** is steric and not electronic. The rate-limiting step of the process is the first Michael attack (**TS17**) with an energy barrier of 8.5 kcal/mol, and further evolution through the only possible species **TS19** fully justifies the obtention of only one isomer with an all-cis configuration.

CONCLUSIONS

The molecular mechanisms for the reaction of nitron ylides with electron-deficient alkenes have been investigated by DFT methods. Both concerted and stepwise mechanisms have been considered. In all cases, the reactions were shown to be stepwise, consisting of an initial Michael attack followed by an intramolecular Mannich-type reaction. Coordination of the lithium atom to the nitron oxygen and carbonyl oxygen atoms in an early step of the reaction promotes both steps efficiently. In our previous experimental work²⁰ we reported that replacing the lithium salts with magnesium or zinc salts resulted in no reaction. Additional calculations are in agreement with this observation and predict that the first rate-limiting step of the cycloaddition is only favored by the lithium cation. In fact, the corresponding zinc- and magnesium-derived transition structures analogous to **TS9** have relative free energies higher than that of **TS9** and lead to unfavorable endergonic formation of the corresponding intermediates **IN2** (see the Supporting Information). The reaction with methyl acrylate can take place through two intermediates associated with di- and tricoordinated lithium models. The tricoordinated model only can lead to the all-cis **2R***,**4R***,**5R*** isomer, whereas the dicoordinated model can lead to isomers having **2R***,**4R***,**5R*** and **2R***,**4S***,**5S*** configurations. Even though both models might be competitive, the calculations correctly predict the experimental observations in which the minor **2R***,**4S***,**5S*** isomer is also obtained. On the other hand, for the reaction of nitron ylides with methyl fumarate and maleate, calculations predict the tricoordinated model as the preferred one, thus explaining that only one isomer is obtained, in full agreement with the experimental findings.

Several levels of theory using B3LYP and M06-2X functionals have been employed, and only those using Truhlar's functional gave successful results. Also, the use of triple- ζ basis sets was crucial for the identification of the stepwise mechanism by means of IRC analyses. Recent studies⁴¹ demonstrated that B3LYP performed very well for geometries, but on the other hand, a very recent report⁴² concludes that M06-2X calculations provide better geometries than B3LYP. Our results indicate that only calculations with M06-2X calculations are consistent with experimental observations and the existing explanation of stereochemical course of the reaction. Hence, it is reasonable to consider that the M06-2X functional, and not B3LYP, represents a valuable method for differentiating concerted and stepwise cycloadditions of ylides and related derivatives. The influence of the solvent on the geometries obtained can be assessed by comparing gas-phase calculations (M06-2X/6-31+G(d) and B3LYP/6-31+G(d) levels) with full optimization considering solvent effects (PCM=THF/M06-2X/6-311+G(d,p) level). In general, no large differences have been observed in the geometries. However, consideration of solvent effects even in single-point calculations (PCM=THF/M06-2X/6-311+G-

(d,p)/B3LYP/6-31+G(d) level) is crucial for obtaining energy values in agreement with experimental findings.

ASSOCIATED CONTENT

Supporting Information

Text, figures, and tables giving the geometries of transition structures **TS1**–**TS8**, absolute (hartrees) and relative (kcal/mol) electronic and free energies at B3LYP/6-31+G(d), M06-2X/6-31+G(d), PCM=THF/B3LYP/6-311+G(d)/B3LYP/6-31+G(d), PCM=THF/M06-2X/6-311+G(d)/B3LYP/6-31+G(d) and PCM=THF/M06-2X/6-311+G(d,p) levels of theory, energy diagrams, IRC analyses, additional calculations with Zn and Mg complexes, and additional calculations with substituted alkenes and Cartesian coordinates of optimized structures. This material is available free of charge via the Internet at <http://pubs.acs.org>.

AUTHOR INFORMATION

Corresponding Author

*P.M.: fax, +34 976 509726; tel, +34 876 553783; e-mail, pmerino@unizar.es.

Notes

The authors declare no competing financial interest.

ACKNOWLEDGMENTS

We thank the following for their support of our programs: the Spanish Ministry of Science and Innovation (Madrid, Spain; Project CTQ2010-19606) and the Government of Aragón (Zaragoza, Spain). A.D.-M. also thanks the Government of Aragón for a predoctoral fellowship. The authors gratefully acknowledge the resources of the supercomputers *Terminus* and *Memento/Cesaraugusta*, and technical expertise and assistance provided by the Institute for Biocomputation and Physics of Complex Systems (BIFI, University of Zaragoza).

REFERENCES

- (1) According to IUPAC (Gold Book) a pericyclic reaction is a process "in which concerted reorganization of bonding takes place throughout a cyclic array of continuously bonded atoms". See: Muller, P. *Pure Appl. Chem.* **1994**, *66*, 1077–1184 (cf. page 1150).
- (2) (a) Firestone, R. A. *Heterocycles* **1987**, *25*, 61–64. (b) Firestone, R. A. *J. Org. Chem.* **1968**, *33*, 2285–2290. (c) Huisgen, R. *J. Org. Chem.* **1976**, *41*, 403–419. (d) Firestone, R. A. *Tetrahedron* **1977**, *33*, 3009–3039. (e) Scaiano, J. C.; Wintgens, V.; Haider, K.; Berson, J. A. *J. Am. Chem. Soc.* **1989**, *111*, 8732–8733. (f) Li, Y.; Padias, A. B.; Hall, H. K., Jr. *J. Org. Chem.* **1993**, *58*, 7049–7058. (g) Klaerner, F.-G.; Krawczyk, B.; Ruster, V.; Deiters, U. K. *J. Am. Chem. Soc.* **1994**, *116*, 7646–7657. (h) Bradley, A. Z.; Kociolek, M. G.; Johnson, R. P. *J. Org. Chem.* **2000**, *65*, 7134–7138.
- (3) (a) de Echaguen, C. O.; Ortuno, R. M. *Tetrahedron Lett.* **1995**, *36*, 749–752. (b) Branchadell, V.; Font, J.; Moglioni, A. G.; de Echaguen, C. O.; Oliva, A.; Ortuno, R. M.; Veciana, J.; Vidal-Gancedo, J. *J. Am. Chem. Soc.* **1997**, *119*, 9992–10003. (c) Lakhdar, S.; Terrier, F.; Vichard, D.; Berionni, G.; El Guesmi, N.; Goumont, R.; Boubaker, T. *Chem. Eur. J.* **2010**, *16*, 5681–5690. (d) Navarro-Vazquez, A.; Alonso-Gomez, J.-L.; Lugtenburg, J.; Cid, M.-M. *Tetrahedron* **2010**, *66*, 3855–3860.
- (4) (a) Yu, Z.-X.; Caramella, P.; Houk, K. N. *J. Am. Chem. Soc.* **2003**, *125*, 15420–15425. (b) Yu, Z.-X.; Houk, K. N. *J. Am. Chem. Soc.* **2003**, *125*, 13825–13830.
- (5) (a) Wagenseller, P. E.; Birney, D. M.; Roy, D. *J. Org. Chem.* **1995**, *60*, 2853–2859. (b) Birney, D. M. *J. Org. Chem.* **1996**, *61*, 243–251. (c) Birney, D. M.; Ham, S.; Unruh, G. R. *J. Am. Chem. Soc.* **1997**, *119*, 4509–4517. (d) Birney, D. M. *Curr. Org. Chem.* **2010**, *14*, 1658–1668.
- (6) Krenske, E. H.; He, S.; Huang, J.; Du, Y.; Houk, K. N.; Hsung, R. P. *J. Am. Chem. Soc.* **2013**, *135*, 5242–5245.

- (7) Merino, P.; Roca-Lopez, D.; Caramella, P.; Tejero, T. *Org. Biomol. Chem.* **2014**, *12*, 517–525.
- (8) (a) Krenske, E. H.; Houk, K. N.; Harmata, M. *Org. Lett.* **2010**, *12*, 444–447. (b) Wang, J.-M.; Li, Z.-M.; Wang, Q.-R.; Tao, F.-G. *Int. J. Quantum Chem.* **2012**, *112*, 809–822. (c) Gonzalez-James, O. M.; Kwan, E. E.; Singleton, D. A. *J. Am. Chem. Soc.* **2012**, *134*, 1914–1917. (d) Arroyo, P.; Picher, M. T.; Domingo, L. R. *J. Mol. Struct. (THEOCHEM)* **2004**, *709*, 45–52. (e) Diez-Martinez, A.; Tejero, T.; Merino, P. *Tetrahedron: Asymmetry* **2010**, *21*, 2934–2943. (f) Lan, Y.; Houk, K. N. *J. Am. Chem. Soc.* **2010**, *132*, 17921–17927. (g) Merino, P.; Tejero, T. *Synlett* **2011**, 1965–1977. (h) Liang, Y.; Liu, S.; Yu, Z.-X. *Synlett* **2009**, 905–909. (i) Liang, Y.; Liu, S.; Xia, Y.; Li, Y.; Yu, Z.-X. *Chem. Eur. J.* **2008**, *14*, 4361–4373.
- (9) (a) Arno, M.; Picher, M. T.; Domingo, L. R.; Andres, J. *Chem.—Eur. J.* **2004**, *10*, 4742–4749. (b) Domingo, L. R.; Picher, M. T.; Arroyo, P.; Saez, J. A. *J. Org. Chem.* **2006**, *71*, 9319–9330. (c) Gassman, P. G.; Gorman, D. B. *J. Am. Chem. Soc.* **1990**, *112*, 8624–8626. (d) Shapiro, N. D.; Toste, F. D. *J. Am. Chem. Soc.* **2008**, *130*, 9244–9245. (e) Domingo, L. R.; Arno, M.; Merino, P.; Tejero, T. *Eur. J. Org. Chem.* **2006**, 3464–3472.
- (10) (a) Houk, K. N.; Li, Y.; Storer, J.; Raimondi, L.; Beno, B. *J. Chem. Soc., Faraday Trans.* **1994**, *90*, 1599–1604. (b) Ajaz, A.; Bradley, A. Z.; Burrell, R. C.; Li, W. H. H.; Daoust, K. J.; Bovee, L. B.; DiRico, K. J.; Johnson, R. P. *J. Org. Chem.* **2011**, *76*, 9320–9328. (c) Qiao, Y.; Chu, T.-S. *J. Org. Chem.* **2011**, *76*, 3086–3095. (d) Saito, T.; Nishihara, S.; Kataoka, Y.; Nakanishi, Y.; Kitagawa, Y.; Kawakami, T.; Yamana, S.; Okumura, M.; Yamaguchi, K. *J. Phys. Chem. A* **2010**, *114*, 12116–12123. (e) Braida, B.; Walter, C.; Engels, B.; Hiberty, P. C. *J. Am. Chem. Soc.* **2010**, *132*, 7631–7637. (f) Xu, L.; Doubleday, C. E.; Houk, K. N. *Angew. Chem., Int. Ed.* **2009**, *48*, 2746–2748. (g) Sakai, S.; Nguyen, M. T. *J. Phys. Chem. A* **2004**, *108*, 9169–9179. (h) Domingo, L. R.; Arno, M.; Contreras, R.; Perez, P. *J. Phys. Chem. A* **2002**, *106*, 952–961. (i) Eichberg, M. J.; Houk, K. N.; Lehmann, J.; Leonard, P. W.; Maerker, A.; Norton, J. E.; Sawicka, D.; Vollhardt, K. P. C.; Whitener, G. D.; Wolff, S. *Angew. Chem., Int. Ed.* **2007**, *46*, 6894–6898. (j) Fernandez, I.; Cossio, F. P.; de Cozar, A.; Lledos, A.; Mascarenas, J. L. *Chem. Eur. J.* **2010**, *16*, 12147–12157.
- (11) (a) Yao, Z.-K.; Yu, Z.-X. *J. Am. Chem. Soc.* **2011**, *133*, 10864–10877. (b) Lage, M. L.; Fernandez, I.; Sierra, M. A.; Torres, M. R. *Org. Lett.* **2011**, *13*, 2892–2895. (c) Kohmoto, S.; Kobayashi, T.; Minami, J.; Ying, X.; Yamaguchi, K.; Karatsu, T.; Kitamura, A.; Kishikawa, K.; Yamamoto, M. *J. Org. Chem.* **2001**, *66*, 66–73. (d) Penoni, A.; Palmisano, G.; Zhao, Y.-L.; Houk, K. N.; Volkman, J.; Nicholas, K. M. *J. Am. Chem. Soc.* **2009**, *131*, 653–661. (e) Nakamura, T.; Takegami, A.; Abe, M. *J. Org. Chem.* **2010**, *75*, 1956–1960.
- (12) Domingo, L. R. *J. Org. Chem.* **1999**, *64*, 3922–3929.
- (13) Domingo, L. R.; Chamorro, E.; Perez, P. *Lett. Org. Chem.* **2010**, *7*, 432–439.
- (14) (a) Freeman, F.; Dang, P.; Huang, A. C.; Mack, A.; Wald, K. *Tetrahedron Lett.* **2005**, *46*, 1993–1995. (b) Das, T. K.; Banerjee, M. *J. Phys. Org. Chem.* **2010**, *23*, 148–155. (c) Chandraprakash, K.; Sankaran, M.; Uvarani, C.; Shankar, R.; Ata, A.; Dallemer, F.; Mohan, P. S. *Tetrahedron Lett.* **2013**, *54*, 3896–3901.
- (15) He, L.; Chen, X.-H.; Wang, D.-N.; Luo, S.-W.; Zhang, W.-Q.; Yu, J.; Ren, L.; Gong, L.-Z. *J. Am. Chem. Soc.* **2011**, *133*, 13504–13518.
- (16) Vivanco, S.; Lecea, B.; Arrieta, A.; Prieto, P.; Morao, I.; Linden, A.; Cossio, F. P. *J. Am. Chem. Soc.* **2000**, *122*, 6078–6092.
- (17) Najera, C.; Retamosa, M. d. G.; Martin-Rodriguez, M.; Sansano, J. M.; de Cozar, A.; Cossio, F. P. *Eur. J. Org. Chem.* **2009**, 5622–5634.
- (18) (a) Hernandez-Toribio, J.; Arrayas, R. G.; Carretero, J. C. *J. Am. Chem. Soc.* **2008**, *130*, 16150–16151. (b) Hernandez-Toribio, J.; Arrayas, R. G.; Carretero, J. C. *Chem. Eur. J.* **2010**, *16*, 1153–1157.
- (19) Castello, L. M.; Najera, C.; Sansano, J. M.; Larranaga, O.; de Cozar, A.; Cossio, F. P. *Org. Lett.* **2013**, *15*, 2902–2905.
- (20) Merino, P.; Tejero, T.; Diez-Martinez, A.; Gueltekin, Z. *Eur. J. Org. Chem.* **2011**, 6567–6573.
- (21) (a) Merino, P. In *Science of Synthesis*; Pawda, A., Bellus, D., Eds.; Georg Thieme Verlag: Stuttgart, New York, 2004; Vol. 27, p 511–580.
- (b) Merino, P. In *Science of Synthesis*; Schaumann, E., Ed.; Georg Thieme Verlag: Stuttgart, New York, 2010; Vol. Update 2010/4, pp 325–403.
- (22) (a) Merino, P.; Anoro, S.; Franco, S.; Merchan, F. L.; Tejero, T.; Tunon, V. *J. Org. Chem.* **2000**, *65*, 1590–1596. (b) Merino, P.; Mates, J. A.; Revuelta, J.; Tejero, T.; Chiacchio, U.; Romeo, G.; Iannazzo, D.; Romeo, R. *Tetrahedron: Asymmetry* **2002**, *13*, 173–190.
- (23) (a) Merino, P.; Lanaspá, A.; Merchan, F. L.; Tejero, T. *Tetrahedron: Asymmetry* **1997**, *8*, 2381–2401. (b) Merino, P.; Revuelta, J.; Tejero, T.; Cicchi, S.; Goti, A. *Eur. J. Org. Chem.* **2004**, 776–782. (c) Delso, I.; Tejero, T.; Goti, A.; Merino, P. *Tetrahedron* **2010**, *66*, 1220–1227.
- (24) (a) Becke, A. D. *J. Chem. Phys.* **1993**, *98*, 5648–5652. (b) Lee, C.; Yang, W.; Parr, R. G. *Phys. Rev. B* **1988**, *37*, 785–789.
- (25) Zhao, Y.; Truhlar, D. G. *Acc. Chem. Res.* **2008**, *41*, 157–167.
- (26) (a) Ditchfield, R.; Hehre, W. J.; Pople, J. A. *J. Chem. Phys.* **1971**, *54*, 724–728. (b) Hehre, W. J.; Ditchfield, R.; Pople, J. A. *J. Chem. Phys.* **1972**, *56*, 2257–2261. (c) Hariharan, P. C.; Pople, J. A. *Theor. Chim. Acta* **1973**, *28*, 213–222. (d) Rassolov, V. A.; Pople, J. A.; Ratner, M. A.; Windus, T. L. *J. Chem. Phys.* **1998**, *109*, 1223–1229. (e) Rassolov, V. A.; Ratner, M. A.; Pople, J. A.; Redfern, P. C.; Curtiss, L. A. *J. Comput. Chem.* **2001**, *22*, 976–984.
- (27) (a) Schlegel, H. B. *J. Comput. Chem.* **1982**, *3*, 214218. (b) Schlegel, H. B. In *Modern Electronic Structure Theory*; Yarkony, D. R., Ed.; World Scientific Publishing: Singapore, 1994.
- (28) (a) Fukui, K. *J. Phys. Chem.* **1970**, *74*, 4161–4163. (b) Fukui, K. *Acc. Chem. Res.* **1981**, *14*, 363–368.
- (29) (a) González, C.; Schlegel, H. B. *J. Phys. Chem.* **1990**, *94*, 5523–5527. (b) González, C.; Schlegel, H. B. *J. Chem. Phys.* **1991**, *95*, 5853–5860.
- (30) Wong, M. W.; Wiberg, K. B.; Frish, M. J. *J. Chem. Phys.* **1991**, *95*, 8991–8998.
- (31) (a) Tomasi, J.; Persico, M. *Chem. Rev.* **1994**, *94*, 2027–2094. (b) Cossi, M.; Barone, V.; Cammi, R.; Tomasi, J. *J. Chem. Phys. Lett.* **1996**, *255*, 327–335. (c) Cossi, M.; Scalmani, G.; Rega, N.; Barone, V. *J. Chem. Phys.* **2002**, *117*, 43–54.
- (32) (a) Domingo, L. R.; Gil, S.; Mestres, R.; Picher, M. T. *Tetrahedron* **1996**, *52*, 11105–11112. (b) Domingo, L. R.; Gil, S.; Mestres, R.; Picher, M. T. *Tetrahedron* **1995**, *51*, 7207–7214.
- (33) Frisch, M. J.; Trucks, G. W.; Schlegel, H. B.; Scuseria, G. E.; Robb, M. A.; Cheeseman, J. R.; Scalmani, G.; Barone, V.; Mennucci, B.; Petersson, G. A.; Nakatsuji, H.; Caricato, M.; Li, X.; Hratchian, H. P.; Izmaylov, A. F.; Bloino, J.; Zheng, G.; Sonnenberg, J. L.; Hada, M.; Ehara, M.; Toyota, K.; Fukuda, R.; Hasegawa, J.; Ishida, M.; Nakajima, T.; Honda, Y.; Kitao, O.; Nakai, H.; Vreven, T.; Montgomery, J. A., Jr.; Peralta, J. E.; Ogliaro, F.; Bearpark, M.; Heyd, J. J.; Brothers, E.; Kudin, K. N.; Staroverov, V. N.; Kobayashi, R.; Normand, J.; Raghavachari, K.; Rendell, A.; Burant, J. C.; Iyengar, S. S.; Tomasi, J.; Cossi, M.; Rega, N.; Millam, J. M.; Klene, M.; Knox, J. E.; Cross, J. B.; Bakken, V.; Adamo, C.; Jaramillo, J.; Gomperts, R.; Stratmann, R. E.; Yazyev, O.; Austin, A. J.; Cammi, R.; Pomelli, C.; Ochterski, J. W.; Martin, R. L.; Morokuma, K.; Zakrzewski, V. G.; Voth, G. A.; Salvador, P.; Dannenberg, J. J.; Dapprich, S.; Daniels, A. D.; Farkas, Ö.; Foresman, J. B.; Ortiz, J. V.; Cioslowski, J.; Fox, D. J. *Gaussian 09. Rev. A1*; Gaussian, Inc., Wallingford, CT, 2009.
- (34) Legault, C. Y. *CYLView, 1.0b*; Université de Sherbrooke, 2009; <http://www.cylview.org>.
- (35) In the original paper the absolute configurations were 2R*,4R*,5S* and 2R*,4S*,5R* because an aromatic substituent (instead of a methyl) is present at the 5-position of the pyrrolidine ring.
- (36) For details on IRC analyses see the Supporting Information
- (37) Neumann, F.; Lambert, C.; Schleyer, P. v. R. *J. Am. Chem. Soc.* **1998**, *120*, 3357–3370.
- (38) (a) Merino, P. C. R. *Chim.* **2005**, *8*, 775–788. (b) Merino, P.; Franco, S.; Merchan, F. L.; Tejero, T. *Synlett* **2000**, 442–454.
- (39) (a) Merino, P.; Tejero, T. *Tetrahedron* **2001**, *57*, 8125–8128. (b) Merino, P.; Mannucci, V.; Tejero, T. *Tetrahedron* **2005**, *61*, 3335–3347. (c) Delso, I.; Marca, E.; Mannucci, V.; Tejero, T.; Goti, A.; Merino, P. *Chem. Eur. J.* **2010**, *16*, 9910–9919.

- (40) (a) Hayes, C. J.; Simpkins, N. S. *Org. Biomol. Chem.* **2013**, *11*, 8458–8462. (b) Abbotto, A.; Streitwieser, A.; Schleyer, P. v. R. *J. Am. Chem. Soc.* **1997**, *119*, 11255–11268.
- (41) Simon, L.; Goodman, J. M. *Org. Biomol. Chem.* **2011**, *9*, 689–700.
- (42) Linder, M.; Brinck, T. *Phys. Chem. Chem. Phys.* **2013**, *15*, 5108–5114.